# INTEGRATE THERMAL MODULES FOR COOLING SILICON AND SILICON CARBIDE POWER MODULES


G. Larry Roderick
k Technology Corporation
2000 Cabot Blvd West, Suite 150
Langhorne, PA 19047
email: roderick@k-technology.com

Terence Burke, Ghassan Khalil
U.S. Army TARDEC
Warren, MI 48397
email: terence.burke@us.army.mil


## INTRODUCTION

A primary limiting factor of solid state converters is thermal management. If chips run too hot, the life of the converter can be drastically shortened. For armored applications weight, size, and cooling temperatures are critical. The objective here in is to use high-conductivity graphite in integrated thermals modules (ITMs) to effectively cool silicon (Si) IGBTs, Si diodes and Silicon Carbide (SiC) diodes.

For a basis of comparing the performance of the ITMs, we are using the Semikron 100 kW SKAI inverter (fig 1) to quantify and generate loads. In Semikron's standard SKAI inverter, there are 12 IGBT's and 6 Silicon diodes. Advanced thermal management techniques are being developed for Semikron's standard SKAI as well as one that uses Silicon Carbide (SiC) diodes. For the later case, as part of this program, Semikron assembled the converter using the SiC diodes. Both the standard and SiC diode converters are being evaluated with different ITMs to enable higher temperature fluids for cooling to enable smaller fluid-to-air heat exchangers for under-armor applications in military vehicles. In addition, for simpler ITM configurations, the ITMs may find cost effective commercial applications.

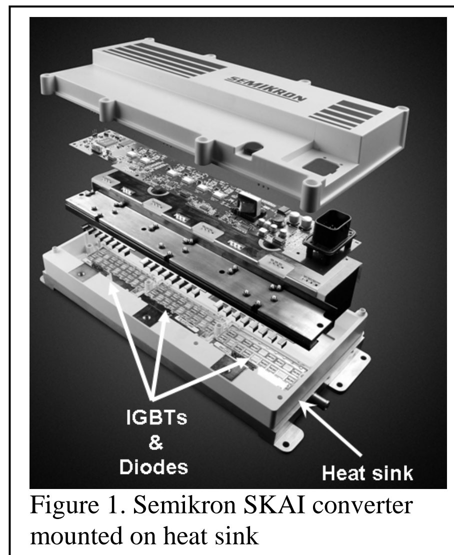

Figure 1. Semikron SKAI converter mounted on heat sink

Notice in figure 1 that the SKAI invert sits on a standard heat sink aluminum heat sink. The heat sink is made of aluminum with pinned fins. As will be shown in following figures, the cooling channel is located directly under the IGBT's and Diodes for three electrical phases. The approach taken herein, is to replace the standard heat sink with an Integrated Thermal Module (ITM) that uses advanced pyrolytic graphite (APG) for more effective heat transfer. The graphite at room temperature has thermal

<table>
<tr><td colspan="5">Report Documentation Page</td><td colspan="2">Form Approved<br>OMB No. 0704-0188</td></tr>
<tr><td colspan="7">Public reporting burden for the collection of information is estimated to average 1 hour per response, including the time for reviewing instructions, searching existing data sources, gathering and maintaining the data needed, and completing and reviewing the collection of information. Send comments regarding this burden estimate or any other aspect of this collection of information, including suggestions for reducing this burden, to Washington Headquarters Services, Directorate for Information Operations and Reports, 1215 Jefferson Davis Highway, Suite 1204, Arlington VA 22202-4302. Respondents should be aware that notwithstanding any other provision of law, no person shall be subject to a penalty for failing to comply with a collection of information if it does not display a currently valid OMB control number.</td></tr>
<tr><td colspan="2">1. REPORT DATE<br>11 JUN 2007</td><td colspan="3">2. REPORT TYPE<br>N/A</td><td colspan="2">3. DATES COVERED<br>-</td></tr>
<tr><td colspan="5" rowspan="3">4. TITLE AND SUBTITLE<br>Integrate Thermal Modules for Cooling Silicon and Silicon Carbide Power Modules</td><td colspan="2">5a. CONTRACT NUMBER</td></tr>
<tr><td colspan="2">5b. GRANT NUMBER</td></tr>
<tr><td colspan="2">5c. PROGRAM ELEMENT NUMBER</td></tr>
<tr><td colspan="5" rowspan="3">6. AUTHOR(S)<br>G. Larry Roderick; Terence Burke; Ghassan Khalil</td><td colspan="2">5d. PROJECT NUMBER</td></tr>
<tr><td colspan="2">5e. TASK NUMBER</td></tr>
<tr><td colspan="2">5f. WORK UNIT NUMBER</td></tr>
<tr><td colspan="5">7. PERFORMING ORGANIZATION NAME(S) AND ADDRESS(ES)<br>US Army RDECOM-TARDEC 6501 E 11 Mile Rd Warren, MI 48397-5000</td><td colspan="2">8. PERFORMING ORGANIZATION REPORT NUMBER<br>17103</td></tr>
<tr><td colspan="5" rowspan="2">9. SPONSORING/MONITORING AGENCY NAME(S) AND ADDRESS(ES)</td><td colspan="2">10. SPONSOR/MONITOR’S ACRONYM(S)<br>TACOM/TARDEC</td></tr>
<tr><td colspan="2">11. SPONSOR/MONITOR’S REPORT NUMBER(S)<br>17103</td></tr>
<tr><td colspan="7">12. DISTRIBUTION/AVAILABILITY STATEMENT<br>Approved for public release, distribution unlimited</td></tr>
<tr><td colspan="7">13. SUPPLEMENTARY NOTES<br>Presented at the 7th International All Electric Combat Vehicle Conference, June 11-13, 2007, Stockholm, Sweden, The original document contains color images.</td></tr>
<tr><td colspan="7">14. ABSTRACT</td></tr>
<tr><td colspan="7">15. SUBJECT TERMS</td></tr>
<tr><td colspan="3">16. SECURITY CLASSIFICATION OF:</td><td rowspan="2">17. LIMITATION OF ABSTRACT<br>SAR</td><td rowspan="2">18. NUMBER OF PAGES<br>8</td><td colspan="2" rowspan="2">19a. NAME OF RESPONSIBLE PERSON</td></tr>
<tr><td>a. REPORT<br>unclassified</td><td>b. ABSTRACT<br>unclassified</td><td>c. THIS PAGE<br>unclassified</td></tr>
</table>

conductivities in-plane of $k_x = k_y = 1500$ W/m°K, and through the thickness of about $k_z = 10$W/m°K compared to that of isotropic aluminum of about k= 180 W/m°K. For the work, a combination of analyses, bench tests and motor tests have been performed.

**Heat Loads**

For electric vehicle applications, there are several loading cases for vehicle operation as follows:

1) Normal Operation at High Speed
2) Normal Operation at Low Speed
3) Acceleration at High Speed
4) Acceleration at Low Speed
5) Stall at 0 degree Offset
6) Stall at 30 degree Offset

Of these loading conditions, Case 3 and Case 6 eclipse that others in term of thermal loads. Case 3, Acceleration at High Speed, gives a more uniform heat load on each phase whereas Case 6 has local peak loads for individual IGBT's and diodes. Figure 2 shows specific IGBT and diode heat loads for each of these two cases.

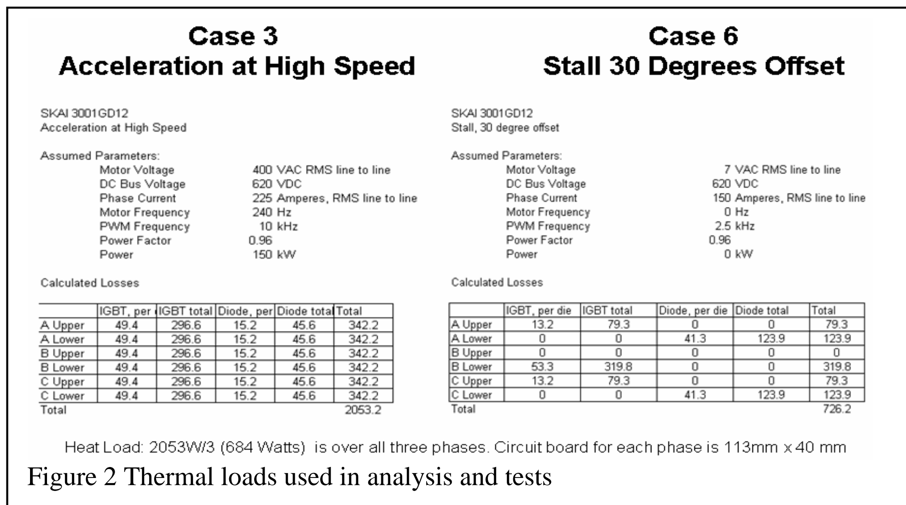

**Case 3**
**Acceleration at High Speed**

SKAI 3001GD12
Acceleration at High Speed

Assumed Parameters:

| | |
|---|---|
| Motor Voltage | 400 VAC RMS line to line |
| DC Bus Voltage | 620 VDC |
| Phase Current | 225 Amperes, RMS line to line |
| Motor Frequency | 240 Hz |
| PWM Frequency | 10 kHz |
| Power Factor | 0.96 |
| Power | 150 kW |

Calculated Losses

| | IGBT, per | IGBT total | Diode, per | Diode total | Total |
|---|---|---|---|---|---|
| A Upper | 49.4 | 296.6 | 15.2 | 45.6 | 342.2 |
| A Lower | 49.4 | 296.6 | 15.2 | 45.6 | 342.2 |
| B Upper | 49.4 | 296.6 | 15.2 | 45.6 | 342.2 |
| B Lower | 49.4 | 296.6 | 15.2 | 45.6 | 342.2 |
| C Upper | 49.4 | 296.6 | 15.2 | 45.6 | 342.2 |
| C Lower | 49.4 | 296.6 | 15.2 | 45.6 | 342.2 |
| Total | | | | | 2053.2 |

**Case 6**
**Stall 30 Degrees Offset**

SKAI 3001GD12
Stall, 30 degree offset

Assumed Parameters:

| | |
|---|---|
| Motor Voltage | 7 VAC RMS line to line |
| DC Bus Voltage | 620 VDC |
| Phase Current | 150 Amperes, RMS line to line |
| Motor Frequency | 0 Hz |
| PWM Frequency | 2.5 kHz |
| Power Factor | 0.96 |
| Power | 0 kW |

Calculated Losses

| | IGBT, per die | IGBT total | Diode, per die | Diode total | Total |
|---|---|---|---|---|---|
| A Upper | 13.2 | 79.3 | 0 | 0 | 79.3 |
| A Lower | 0 | 0 | 41.3 | 123.9 | 123.9 |
| B Upper | 0 | 0 | 0 | 0 | 0 |
| B Lower | 53.3 | 319.8 | 0 | 0 | 319.8 |
| C Upper | 13.2 | 79.3 | 0 | 0 | 79.3 |
| C Lower | 0 | 0 | 41.3 | 123.9 | 123.9 |
| Total | | | | | 726.2 |

Heat Load: 2053W/3 (684 Watts) is over all three phases. Circuit board for each phase is 113mm x 40 mm

Figure 2 Thermal loads used in analysis and tests

**Graphite Material System**

The basic concept of the Integrated Thermal Module approach is to make use of Advanced Pyrolytic Graphite (APG) to improve the performance of the heat sink and to allow the converter to operate with high temperature coolants. k Technology has used the APG in its standard product line, k-Core, for a

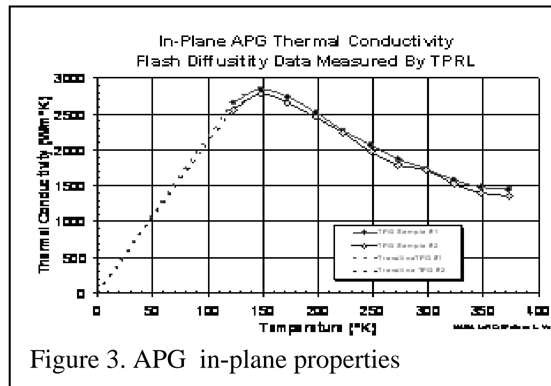


Figure 3. APG in-plane properties

variety of proven applications. It has been qualified and is in use on aircraft, spacecraft, phased array radars and a host of other applications. Figure 3 shows in-plane properties of the APG as a function of temperature. As the figure shows, between 70°K to 350°K the thermal conductivity is higher than 1500 W/m°K. In contrast, the through-the-thickness (TTT) thermal conductivity is about 10 W/m°K. This fact has to be taken into account when designing for some specific applications. Also, the material has little strength, somewhat equivalent to a pencil lead. For that reason, APG is typically is encapsulated with another material such as aluminum to enhance its structural integrity.

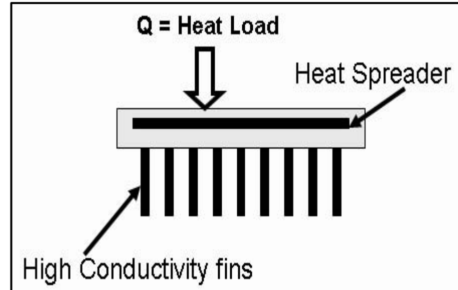


Figure 4. Use of APG in Integrated Thermal Module

**Integrated Thermal Module (ITM)**

Figure 4 shows the ITM concept where the graphite can be used as a heat spreader or a high efficiency fin material. Although simple in concept, there are several design considerations that need to be employed to use the APG effectively for heat sinks and heat exchangers. For example, in some heat spreader applications thermal vias are used to effectively transfer the load into and through the thickness of the spreader. In this effort, several different ITM Configurations are being investigated. Figure 5 shows the various configurations under investigation. The designation k-Core.Al denotes APG encapsulated in aluminum and k-Core.mm designates a CTE matched metal matrix composite encapsulate. The wide plenum opens up a larger flow area. Given improved heat spreaders with k-Core, more fins may be effective in heat transfer and therefore lower the $T_{max}$ in the chips. Moreover, for the same inlet flow relative to the baseline heat sink channel the fluid velocity is lower and could lead to lower pressure drops across the heat sink. All of these ITM configurations are under consideration in the program through analysis, bench tests, and motor tests cooling with propylene glycol and engine oil. Those that appear most effective from the analyses, go through bench tests. In turn, the best two performers from bench tests are tested in motor tests using power modules with and without SiC diodes.

A very simple ITM is one that just replaces the pin fin array with simple plate fins made out of APG. Looking at the bottom of the heat sink (cover removed), Figure 6a shows the standard heat sinks with the pin fin arrays and Figure 6b shows that pin fin array replaced with APG fins. The ITM was also designed to limit heat spreading to get an evaluation of the pins versus APG fins. A test of the effectiveness of the APG fins versus the standard pin fin array was determined by testing each under identical heat loads for several flow conditions for two different cooling fluids: propylene glycol (PG) and engine oil. Even though the inlet flow conditions are identical for both cases, the geometry of the pin fin arrays precipitates a much higher local (pin) convection coefficient than that for simple APG fins. Both the baseline pin fins heatsink and ITM with APG fins were tested using a heater with a 25mm x 100mm heat foot print over the center phase location. As a result, there is effectively a uniform heat load between chip locations. Figure 7 shows the bench test set up.

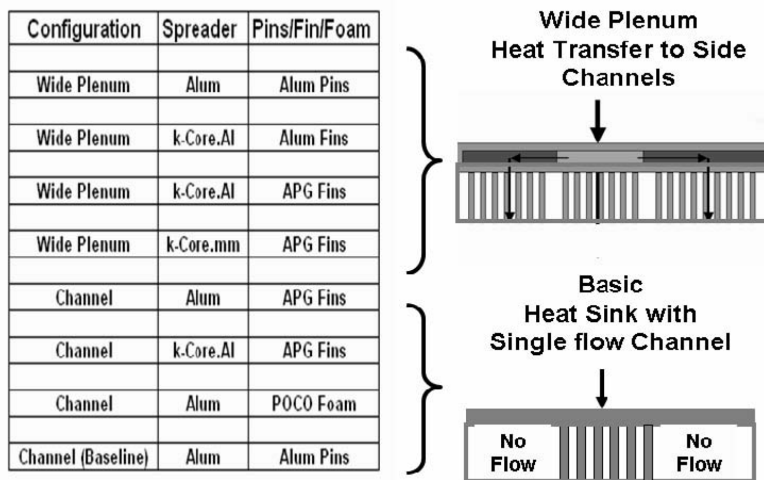

| Configuration | Spreader | Pins/Fin/Foam |
|---|---|---|
| Wide Plenum | Alum | Alum Pins |
| Wide Plenum | k-Core.Al | Alum Fins |
| Wide Plenum | k-Core.Al | APG Fins |
| Wide Plenum | k-Core.mm | APG Fins |
| Channel | Alum | APG Fins |
| Channel | k-Core.Al | APG Fins |
| Channel | Alum | POCO Foam |
| Channel (Baseline) | Alum | Alum Pins |



Figure 5. Integrated Thermal Module (ITM) Configurations

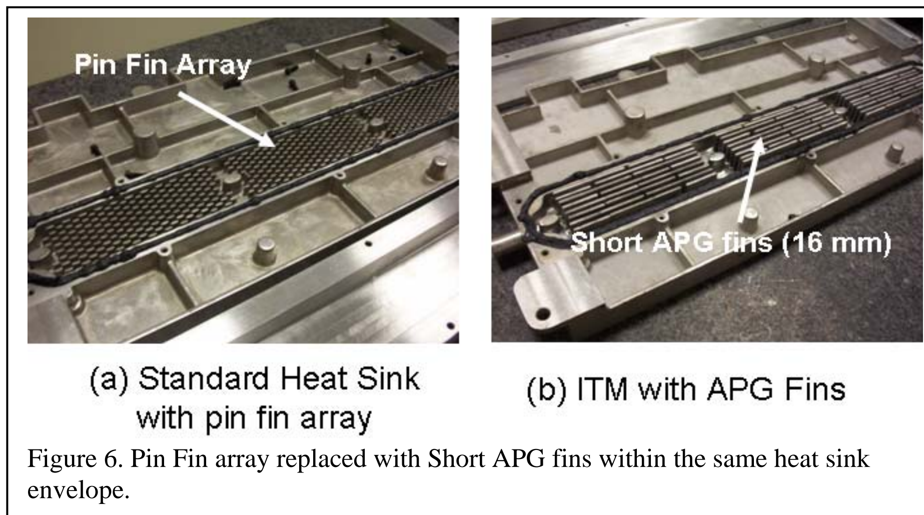


Figure 6. Pin Fin array replaced with Short APG fins within the same heat sink envelope.

There is an array of thermal sensors on the surface of the heat sink around the edge of the heater footprint. Figure 8 shows the results of the bench tests with three different flow rates. As the graph shows, using the propylene glycol and engine oil as coolant shows a temperature reduction, versus the baseline heat sink with pin fins, of about 10°C and 19°, respectively, for a load of about 980W over a 25mm x 100mm footprint. The results clearly shows that the APG fins out perform the aluminum pin fin array.

To investigate the need for heat spreading in the ITM, another series of bench tests were run where the heat block was configured to simulate concentrated heat loads on the chips. To that end, 9mm by 9mm bosses were used on the heat block and data points were taken for the same flow conditions shown in Figure 7. In this case, there was very little difference between the baseline heat sink and the ITM with the APG fins. Consequently, to take advantage of the more effective fins, a heat spreader needs to be

integrated into the ITM configuration to effect good heat transfer from local heating at the chips.

To assess the best placements of the heat spreader in the ITM, three dimensional, orthotropic finite element models of both the baseline and various ITM configurations with heat spreaders were made. Figure 9 shows the prediction of the temperature profile for a typical ITM configuration with loads on diodes and IGBT's as shown in Figure 2.

The FEM model takes into account the stack up of thermal resistance between the chip and the ITM. Convection coefficients used for the analysis are based on similar inlet flow rates for all comparisons, but the local flow configurations are taken into account to calculate respective convection coefficients. For example, for flow rates of 10 liters/min, the convection coefficients calculated from empirical correlations for propylene glycol are twice as high for the baseline pin configuration as for the IPM with the APG fins

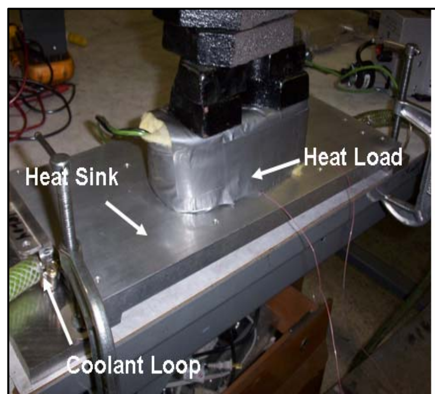


Figure 7. Bench test set up

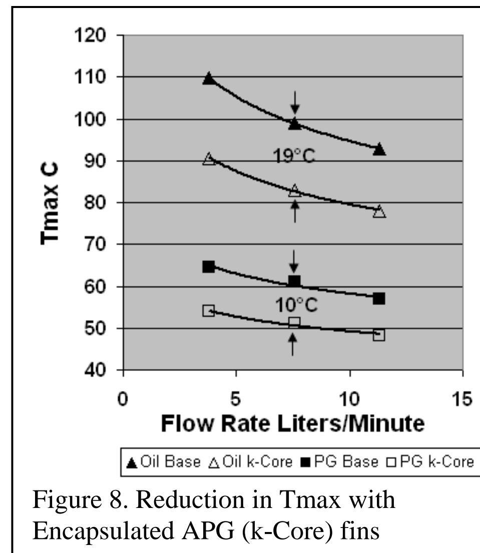


Figure 8. Reduction in Tmax with Encapsulated APG (k-Core) fins

**Silicon Carbide Diodes**

A key objective of the ITM is to cool SiC diodes and SiC MOSFETs in advanced converters. So, there are two baseline SKAI 100kW converters being used for testing. One uses standard Si diodes used in standard Semikron products. The second uses SiC diodes working in conjunction with the Silicon IGBTs. Under a subcontract from k Technology, Semikron integrated Cree SiC diodes into the SKAI converter. For the same motor loads, the SiC diodes have the effect of reducing the waste loads in the IGBT's consequently allowing higher performance of the motor drive. Figure 10 shows the specifications of the Cree SiC diodes used in the SKAI 100. The SiC diodes have the following features: 1200-Volt Schottky Rectifier, zero reverse recovery, zero forward recovery, high-frequency operation, temperature-independent switching behavior, extremely fast switching, and positive temperature coefficient of $V_F$.

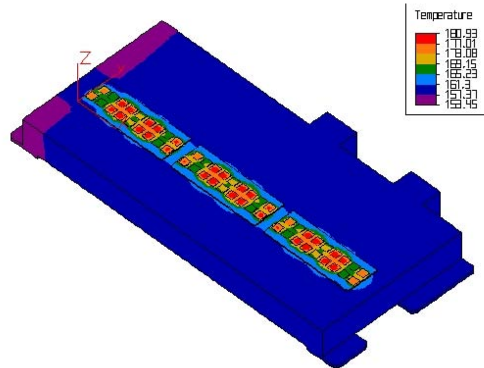


Figure 9.Resultsof 3D, Orthotropic Finite Element Analysis for cooling of IGBT's and Diodes using detailed chip heat loading

**Electrical Characteristics**

| Symbol | Parameter | Typ. | Max. | Unit | Test Conditions | Note |
|---|---|---|---|---|---|---|
| $V_F$ | Forward Voltage | 1.65<br>2.6 | 2.0<br>3.0 | V | $I_F$ = 50 A $T_J$=25°C<br>$I_F$ = 50 A $T_J$=175°C | |
| $I_R$ | Reverse Current | 10<br>50 | 200<br>1000 | μA | $V_R$ = 1200 V $T_J$=25°C<br>$V_R$ = 1200 V $T_J$=175°C | |
| $Q_C$ | Total Capacitive Charge | 305 | | nC | $V_R$ = 500 V, $I_F$ = 50 A<br>di/dt = 500 A/μs<br>$T_J$ = 25°C | |
| C | Total Capacitance | 4500<br>396<br>325 | | pF | $V_R$ = 0 V, $T_J$ = 25°C, f = 1 MHz<br>$V_R$ = 200 V, $T_J$ = 25°C, f = 1 MHz<br>$V_R$ = 400 V, $T_J$ = 25°C, f = 1 MHz | |

Note:
1. Assumes $\theta_{J\text{-}C}$ Thermal Resistance of 0.5°C/W or less.

Figure 10 SiC diodes electrical characteristics

**Motor Testing**

The ultimate test of the ITM for both Si and SiC chips is improved converter operation under motor loads. So, a significant evaluation of the ITMs is for their use in converters used to drive motors. To this end, under subcontract from k Technology, Comprehensive Power is conducting motor tests in their Massachusetts facility. The inverter load tests are performed with high horsepower permanent magnet (PM) motors on back-to-back test stands where there is a converter-motor-converter-generator loop. The motor in the test stand is shown in Figure 11.

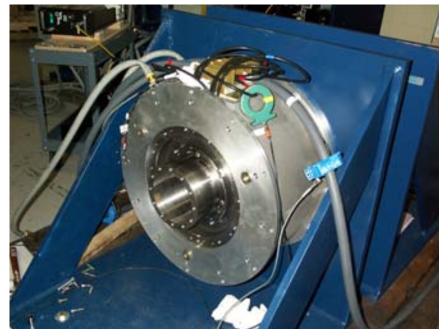

Figure 11. Motor in test stand

For the test operation, there are several features:

- 650 VDC input to the inverter
- 0-480 HZ output to the motor
- Programmable load cycles with full quadrant operation.

In contrast to the bench tests where temperatures are measured on the surface of the ITM, in the motor tests real time temperatures of the IGBT's by calibrating IGBT temperature with the IGBT forward voltage. To this end, a small forward voltage is measured at a small reference current. The voltage decreases with increasing temperature and offsets will vary among wafers. The scale can be calibrated by measurement at zero power. Figure 12 shows the calibration for a 500 amp IGBT. For resolution at higher temperature a higher reference temperature is required. As the forward voltage is measure through the tests, it can be converted in real time to the IGBT temperatures.

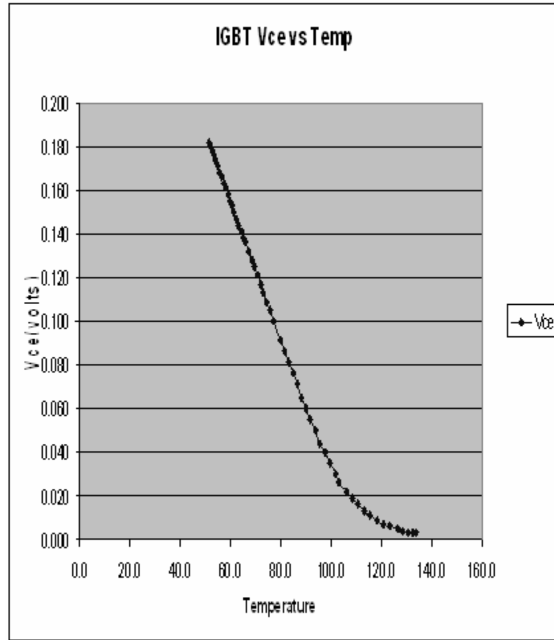


Figure 12. Calibration of IGBT Temperature with $V_{CE}$

There is a matrix of tests planned to fully evaluate the performance of the ITM. Figure 13 below shows the test matrix. The X mark tests that have been completed as of this writing.

| Motor tests X - Completed | Heat sinks | | | | | |
|---|---|---|---|---|---|---|
| | Baseline | | ITM-1 | | ITM-2 | |
| | Engine Oil | Propylene Glycol | Engine Oil | Propylene Glycol | Engine Oil | Propylene Glycol |
| | | | | | | |
| SKAI-Standard | | X | | | | |
| | | | | | | |
| SKAI-SiC Diodes | | X | | | | |
| | | | | | | |

Figure 13. Motor Test Matrix

Motor tests were conducted on the standard SKAI and the SKAI with SiC diodes using propylene glycol for cooling with the standard Semikron baseline heat exchanger. Results showed that the SKAI with SiC diodes reduce the IGBT operating temperature by about 8% over that of the standard SKAI. The 8% benefit obtained by

using SiC diodes is a reduction in the switching losses seen by the opposing IGBT. The reduction in switching losses translates directly into lower temperature. The loss mechanism can be described as follows. When the upper IGBT in a phase is turned off, the current for that phase conducts through the lower diode. When the upper IGBT is turned back on it tries to pull the phase voltage up to the positive rail. The voltage across the diode changes from a forward voltage of around one volt to a reverse blocking voltage of 7-800 volts. As the diode goes from conducting to blocking the forward current stops, and a bit of charge flows in the reverse direction to clear out the junction. The amount of charge is quantified as the Reverse Recovery Charge, and the time it takes to be swept out is called the Reverse Recovery Time. The charge is much higher when the diode is hot. All of this reverse recovery charge flows from the positive rail through the IGBT and diode straight to the negative rail, dissipating an energy equal to the charge times the bus voltage. The power is the energy times the switching frequency. The loss is split between the IGBT and diode, but most of the loss is in the IGBT because the reverse voltage across the diode cannot increase much until the charge is swept out. The SiC diode has a much lower recovery charge (Qr = 305 nC on the data sheet, silicon is ~100x larger). 30 microcoulombs times 800 volts at 10 kHz is 240 watts of loss, reduced to 2.4 watts.

## SUMMARY

Thermal management is an enabling technology for high-power density, three-phase converters using Si(Silicon) or SiC(Silicon Carbide) based power modules. This paper describes a comprehensive analytical/experimental program to assess and demonstrate the viability of using high-conductivity, advanced pyrolytic graphite (APG) in an Integrated Thermal Module (ITM) to cool chips in converters. The Semikron 100kW SKAI converter with Silicon IGBTs and diodes with a standard heat was used as a baseline. Against the baseline, both a Semikron SKAI with SiC diodes and various ITMS were developed to replace the standard baseline heat sink.

As a start for the analysis and tests, individual IGBT and Diode converter heat loads were calculated for a 100 kW permanent magnet motor operation in six different loading cases. The most severe of these for uniform heating and peak heating were "Acceleration at High Speed" and "Stall at a 30 degree Offset".

ITMs were developed that used APG for fins and heat spreaders encapsulated in aluminum and metal matrix composites for both a standard 40mm plenum and a 120mm wide plenum. The ITMs were analyzed under several different inlet flow rates for both propylene glycol (PG) and engine oil coolant. To this end, three-dimensional, orthotropic finite element analyses were performed. In the analyses, convection coefficients for pin arrays and APG fins were calculated using semi-empirical correlations for the various internal flow characteristics.

As of this writing, the first series of bench tests for a uniform heat load on the various ITM modules were conducted and showed 10°C and 20°C reduction in temperature for PG and engine oil coolant, respectively, compared to the baseline, pin-finned heat sink. Bench tests are currently being conducted using local simulated heat loads for IGBTs and diodes.

To evaluate the ITMs and SiC diodes a motor test stand is being used. So far, the baseline SKAI and the SKAI with SiC diodes have been tested using the standard heat sink. During the motor tests, IGBTs heat loads were monitored real time through a correlation of IGBT voltage and temperatures. The results show that the IGBTs in conjunction with SiC diodes run about 8% cooler than the baseline SKAI with silicon diodes.